

MOISTURE EFFECTS OF UNSATURATED POROUS SOILS ON INDOOR AIR ENTHALPY

Gerson Henrique dos Santos and Nathan Mendes
Pontifical Catholic University of Paraná- PUCPR
Thermal Systems Laboratory
R. Imaculada Conceição, 1155, 80.215-901 - Curitiba-PR, Brazil
gerson.santos@pucpr.br

ABSTRACT

A mathematical model applied to building hygrothermal behavior analysis is described in this paper. We have used a lumped approach to model the room air temperature and humidity and a multi-layer model in finite volumes for the building envelope. The capacitance model allows studying the dynamic performance of both humidity and temperature of a building zone when it is submitted to the different climatic factors. In the results section, we show the moisture effects on the heat and mass transfer through the floor and ground. The methodology presented for the soil and floor model was based on the Philip and De Vries theory. The governing equations were discretized in finite volumes and a 3-D model was used for ground and floor.

INTRODUCTION

Since the seventies, due to the worldwide energy crisis, some countries have adopted a severe legislation aiming to promote energy efficiency of equipment and buildings. In this context, to evaluate the building performance with thermal parameters, several codes have been developed. However, most of those codes do not take into account the moisture presence within building envelopes and present some simplifications on their calculation routines by not considering the three-dimensional aspects of heat and moisture transfer via the ground and floor and have not focused these effects on highly-capillary soils. The moisture in the furniture and envelope of buildings implies an additional mechanism of transport absorbing or releasing latent heat of vaporization, affecting the hygrothermal building performance and causing mold growth.

Some building physics studies involving the pure conduction heat transfer through the ground can be found in the literature. The first experimental study concluded that the heat loss through the ground is proportional to the size of its perimeter. However, Bahnfleth (1989) observed that the area and shape must be taken into account as well.

Davies *et al.* (1995), using the finite-volume approach, compared multidimensional models and

observed that the use of three-dimensional simulation provides better prediction of building temperature and heating loads than two-dimensional simulation, when these results are compared with experimental data.

In the works mentioned above, the conductivity and the thermal capacity are considered constant and the moisture effect is ignored. However, the presence of moisture in the ground implies an additional mechanism of transport: in the pores of unsaturated soil, liquid water evaporates at the warm side, absorbing latent heat of vaporization, while, due to the vapor-pressure gradient, vapor condenses on the coldest side of the pore, releasing latent heat of vaporization (Deru and Kirkpatrick, 2002). This added or removed latent heat can cause great discrepancies on the prediction of room air temperature and relative humidity, when compared to values obtained by pure conduction heat transfer (Mendes, 1997).

In addition, Janssen *et al.* (2002) elaborated an analysis of heat loss through a basement and concluded that the combined heat and mass transfer in ground can not be ignored for the heat flow calculation through the building foundation

In soil simulation, some parameters such as the boundary conditions, initial conditions, simulation time period (including warm-up), simulation time step and grid refinement have to be carefully chosen and combined in order to reach accuracy without using excessive computational processing.

In this way, a mathematical model is presented in order to test the hygrothermal performance of buildings by considering the combined three-dimensional heat and moisture transport through the ground for capillary unsaturated porous soils. Heat diffusion through building envelope (walls and roof) was calculated by using the Fourier's law.

The importance of considering a three-dimensional approach for the soil domain for low-rise buildings was verified by Santos and Mendes (2004a), using a simply conductive model for ground heat transfer calculation. For ensuring numerical stability in the present model, the linearized set of equations was obtained by using the finite-volume method and the

MultiTriDiagonal-Matrix Algorithm (Mendes *et al.*, 2002) to solve the 3-D soil and floor model.

The room can be submitted to loads of solar radiation, inter-surface long wave radiation, convection, infiltration and internal gains from light, equipment and people. A lumped approach for energy and water vapor balances is used to calculate the room air temperature and relative humidity.

MATHEMATICAL MODEL

The physical problem is divided into three domains: ground, building envelope (walls and roof) and room air. At the external surfaces, the heat transfer due to short wave radiation and convection were considered as boundary conditions and the long-wave radiation losses were taken into account only at horizontal surfaces, i. e., ground and roof. At the internal surfaces, besides the convection heat transfer, long-wave radiation exchange between the surfaces was considered and for the ground and floor a combined heat and mass transfer model was used.

Soil and Floor Domain

The governing equations, based on the theory of Philip and De Vries (1957), to model heat and mass transfer through porous media, are given by Eqs. (1) and (2). The energy conservation equation is written in the form

$$\rho_0 c_m(T, \theta) \frac{\partial T}{\partial t} = \nabla \cdot (\lambda(T, \theta) \nabla T) - L(T) (\nabla \cdot \mathbf{j}_v) \quad (1)$$

and the mass conservation equation as

$$\frac{\partial \theta}{\partial t} = -\nabla \cdot \left(\frac{\mathbf{j}}{\rho_l} \right), \quad (2)$$

The total 3-D vapor flow (\mathbf{j}) - given by summing the vapor flow (\mathbf{j}_v) and the liquid flow (\mathbf{j}_l) - can be described as

$$\begin{aligned} \frac{\mathbf{j}}{\rho_l} = & - \left(D_T(T, \theta) \frac{\partial T}{\partial x} + D_\theta(T, \theta) \frac{\partial \theta}{\partial x} \right) \mathbf{i} - \\ & \left(D_T(T, \theta) \frac{\partial T}{\partial y} + D_\theta(T, \theta) \frac{\partial \theta}{\partial y} \right) \mathbf{j} , \\ & - \left(D_T(T, \theta) \frac{\partial T}{\partial z} + D_\theta(T, \theta) \frac{\partial \theta}{\partial z} + \frac{\partial K_g}{\partial z} \right) \mathbf{k} \end{aligned} \quad (3)$$

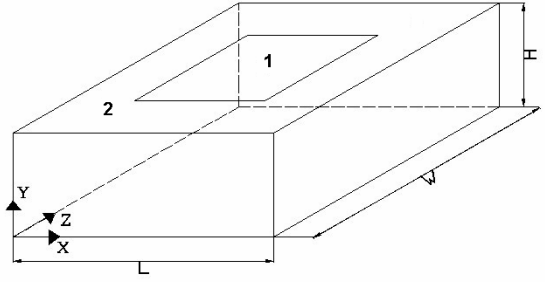


Figure 1: Physical domain for ground and floor.

Figure 1 shows the physical domain. According to Fig. 1, the boundary conditions, for the most generic case (3-D), can be mathematically expressed as:

Surface1 (in contact with internal air):

$$\begin{aligned} \left(\lambda_f(T, \theta) \frac{\partial T}{\partial y} \right)_{y=H} + (L(T) j_v)_{y=H} = \\ h_f (T_{int} - T_{y=H}) + \sum_{i=1}^m f_v \varepsilon_f \sigma (T_{sur}^4 - T_{y=H}^4) + \\ L(T) h_{mf} (\rho_{v,int} - \rho_{v,y=H}) \end{aligned} \quad (4)$$

Surface 2 (in contact with external air):

$$\begin{aligned} \left(\lambda_s(T, \theta) \frac{\partial T}{\partial y} \right)_{y=H} + (L(T) j_v)_{y=H} = \\ h_s (T_{ext} - T_{y=H}) + \alpha_s q_r + L(T) h_{ms} (\rho_{v,ext} - \rho_{v,y=H}), \\ - \varepsilon_s R_{lw} \end{aligned} \quad (5)$$

where $h(T_{\infty} - T_{y=H})$ represents the heat exchanged by convection with the external air, described by the surface conductance h , $\alpha_s q_r$ is the absorbed short-wave radiation and $L(T) h_{ms} (\rho_{v,\infty} - \rho_{v,y=H})$, the phase-change energy term. The long-wave radiation loss is defined as R_{lw} (W/m^2) and ε is the surface emissivity. The solar absorptivity is represented by α and the mass convection coefficient by h_m , which is related to h by the Lewis' relation.

Similarly, the mass balance at the upper surface is written as

$$\begin{aligned} \left(D_{\theta f}(T, \theta) \frac{\partial \theta}{\partial y} + D_{Tf}(T, \theta) \frac{\partial T}{\partial y} \right)_{y=H} = \\ \frac{h_{mf}}{\rho_l} (\rho_{v,int} - \rho_{y=H}) \end{aligned} \quad (6)$$

for surface1 (in contact with internal air), and as

$$\left(D_{\theta}(T, \theta) \frac{\partial \theta}{\partial y} + D_{T_s}(T, \theta) \frac{\partial T}{\partial y} \right)_{y=H} = \frac{h_{ms}}{\rho_l} (\rho_{v,ext} - \rho_{y=H}) \quad (7)$$

for surface 2 (in contact with external air).

The other soil domain surfaces were all considered adiabatic and impermeable.

Building Envelope Domain

As the scope of this work is to analyze the coupled three-dimensional heat and moisture transfer through the ground, a simple one-dimensional conductive heat transfer model was considered for the building envelope including walls and roof. In this way, the internal surface temperature is calculated by an energy balance equation, in an elemental control volume, using the Fourier's law:

$$\rho c \frac{\partial T}{\partial t} = \lambda \frac{\partial^2 T}{\partial x^2} \quad (9)$$

On the external side of the room, the walls, roof, doors and windows are exposed to solar radiation and to convection heat transfer. In this way, the external boundary condition ($x=0$) can be mathematically expressed as:

$$-\left(\lambda_w \frac{\partial T}{\partial x} \right)_{x=0} = h_{ext}(T_{ext} - T_{x=0}) + \alpha_w q_r \quad (8)$$

On the internal side ($x=L$), the inter-surface long-wave radiation was included as:

$$\left(\lambda_w \frac{\partial T}{\partial x} \right)_{x=L} = h_{int}(T_{int} - T_{x=L}) + \sum_{i=1}^m f_v \varepsilon_w \sigma (T_{sur}^4 - T_{x=L}^4) \quad (9)$$

On the other hand, for the roof, long-wave radiation losses were considered (R_{lw}) so that Eq. (8) has assumed the following form:

$$-\left(\lambda_{roof} \frac{\partial T}{\partial x} \right)_{x=0} = h_{roof}(T_{ext} - T_{x=0}) + \alpha_{roof} q_r - \varepsilon_{roof} R_{lw} \quad (10)$$

It has been assumed that surrounding surfaces that face the building envelope and the building envelope surfaces are nearly at the same temperature. In this way, the long-wave radiation term was only considered in Eq. (10).

The solar radiation (direct, reflected and diffuse) came from models presented by ASHRAE (1997) and are conveniently projected to each surface considered in both envelope and soil domains. In this way, the numerical value of " q_r ", shown in Eqs.

(1-10), is modified according to the projection of the solar beam at each simulation time step.

Internal Air Domain

The present work uses a dynamic model for analysis of hygrothermal behavior of a room without HVAC system. Thus, a lumped formulation for both temperature and water vapor is adopted. Equation (11) describes the energy conservation equation applied to a control volume that involves the room air, which is submitted to loads of conduction, convection, short-wave solar radiation, inter-surface long-wave radiation and infiltration:

$$\dot{E}_t + \dot{E}_g = \rho_{air} c_{air} V_{air} \frac{dT_{int}}{dt} \quad (11)$$

The term \dot{E}_t , on the energy conservation equation, includes loads associated to the building envelope (sensible heat) and latent conduction from floor, fenestration (conduction and solar radiation), and openings (ventilation and infiltration).

The sensible heat released by the building envelope and floor is calculated as

$$Q_S(t) = \sum_{i=1}^m h_{int} A_i [T_{x=e}(t) - T_{int}(t)] \quad (12)$$

for the sensible conduction load and as

$$Q_{floor}(t) = \sum_{j=1}^n L(T_{Y=H}(t)) h_{mf} A_{j,f} [\rho_{v,int}(t) - \rho_{v,f}(t)] \quad (13)$$

for the latent load from floor.

In terms of water vapor mass balance, different contributions were considered: ventilation, infiltration, internal generation, people breath and floor surface. In this way, the lumped formulation becomes:

$$(\dot{m}_{inf} + \dot{m}_{vent})(W_{ext} - W_{int}) + \dot{m}_b + \dot{m}_{ger} + \sum_{j=1}^n h_D A_{j,f} [W_{v,f} - W_{int}] = \rho_{air} V_{air} \frac{dW_{int}}{dt} \quad (14)$$

The water-vapor mass flow from the people breath is calculated as shown in ASHRAE (1997), which takes into account the room air temperature, humidity ratio and physical activity as well.

Santos and Mendes (2004b) presented and discussed different numerical methods used to integrate the differential governing equations in the air domain (Eqs. 11 and 14), showing the results in terms of accuracy and computer run time.

SIMULATION PROCEDURE

A C-code was elaborated for the prediction of the building hygrothermal performance. For the simulation, a 25-m² single-zone building with 2 windows (single glass layer) and 1 door were used. For the conduction load calculation, 0.19-m thick walls composed of 3 layers were used: mortar (2 cm), brick (15 cm) and mortar (2cm). In those typical Brazilian walls, the contact resistance between two different layers was not considered.

The differential equations of energy conservation for each node of the building envelope (walls and roof) were discretized by using the finite-volume method (Patankar, 1980), with a central difference scheme, a uniform grid and a fully-implicit approach. The solution of the set of algebraic equations was obtained by using the TDMA (TriDiagonal-Matrix Algorithm).

For the building envelope, a 1-D model was considered since the temperature gradients are much higher on the normal direction. The thermophysical properties of the building envelope materials were gathered from Incropera (1998) and considered.

For the presented single-zone building, a 0.35-m concrete floor was considered within the soil domain as it can be seen in Fig. 2. The governing partial differential equations were discretized by using the control-volume formulation method (Patankar, 1980). The spatial interpolation method used is the control-difference scheme (CDS) and the time derivatives are integrated using a fully-implicit approach. In the 3-D model for the ground and floor, an amount of 9,261 nodes were used.

The MTDMA (MultiTriDiagonal-Matrix Algorithm; Mendes *et al.*, 2002) was used to solve a 3-D model to describe the physical phenomena of the strongly coupled heat and mass transfer in porous soils. In this algorithm, the dependent variables are obtained simultaneously, avoiding numerical divergence caused by the evaluation of coupled terms from previous iteration values.

In this work, the properties of soil (sandy silt soil) strongly affected by temperature and moisture content were taken from Oliveira *et al.* (1993).

In this work, internal generation of both energy and mass was not considered and an infiltration rate of 1 L/s was adopted. The Sun effect (short-wave radiation) on the ground was considered on East side until noon, and on West side, from noon until 6 pm. On North side, solar radiation was considered during all day and at no moment on the South side

as the building is located in the city of Curitiba (South of Brazil at a latitude of -25.4°).

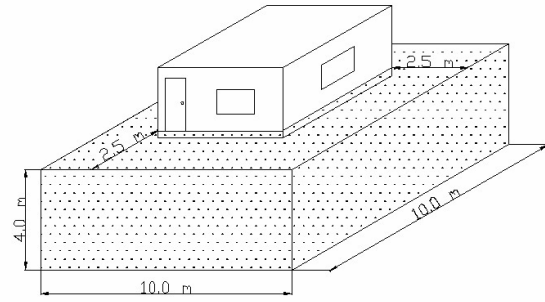


Figure 2: Dimensions of the soil and floor domain used in the simulation.

The external climate was represented by Eqs. [15-17] for temperature, relative humidity and solar radiation, respectively. It was considered a yearly average temperature of 20 °C with a daily variation of 5°C. A yearly variation of 5°C was considered for the peak values. For the external relative humidity, a daily variation between 50 % and 70 % was considered. A yearly variation on the peak values is not used in this case.

The value for total solar radiation (direct + diffuse) is valid between 6 am and 6 pm, with a peak value at noon, and, elsewhere, it is equal to zero.

$$T_{ext} = 20 + 5 \sin\left(\pi + \frac{\pi t}{31536000}\right) + 5 \sin\left(\pi + \frac{\pi t}{43200}\right) \quad (15)$$

$$\phi_{ext} = 0.60 - 0.10 \sin\left(\pi + \frac{\pi t}{43200}\right) \quad (16)$$

$$q_{rad} = 300 + 100 \sin\left(\pi + \frac{\pi t}{31536000}\right) \quad (17)$$

$$\cdot \sin\left(\frac{3\pi}{2} + \frac{\pi t}{43200}\right)$$

RESULTS

The boundary conditions, the pre-simulation time period (warm-up), the size of the physical domain, the simulation time step, the grid refinement, the convergence errors and the required computer run time are important simulation parameters, which have to be chosen very carefully in order to accurately predict temperature and moisture content profiles in soils under different sort of weather data. Santos and Mendes (2005) showed in details the sensitivity analysis for these cases.

For analyzing the moisture effects of unsaturated porous soil on the indoor air thermodynamic state, a 3-D conductive heat transfer model (named “Pure Conduction”) has been compared to the 3-D combined heat and moisture transfer model (called “With Moisture”) presented previously in this paper.. For both “Pure Conduction” and “With Moisture” cases, sinusoidal functions (Eqs. 15-17) have been considered to represent the weather. In the soil domain of the building located in the city of Curitiba-Brazil (South latitude of 25.4°), a constant convection heat transfer coefficient of 10 W/m²K, an absorptivity of 0.5 and a constant long-wave radiation loss of 30 W/m² have been considered for boundary condition equation at the upper soil surface . The other soil surfaces have been considered adiabatic and impermeable.

Moisture Effects on Indoor Air

A warm-up period of 2 years has been used throughout the moisture effects comparative analysis. A sandy-silt soil, has been chose for the simulation and its hygrothermal properties have been gathered from Oliveira et al. (1993), while for a single-layer mortar floor, the properties have been compiled from Perrin (1985)..

Constant convection heat transfer coefficients of 12 W/m²K and 3 W/m²K have been used at the external and internal surfaces, respectively.. A constant 30-W/m² long-wave radiation heat transfer loss through the roof has been considered, while a 0.3 absorptivity coefficient was applied for the short-wave radiation for all building surfaces.

In Figs. 3-6, a temperature of 20 °C and a volumetric moisture content of 4 % have been considered as initial conditions.

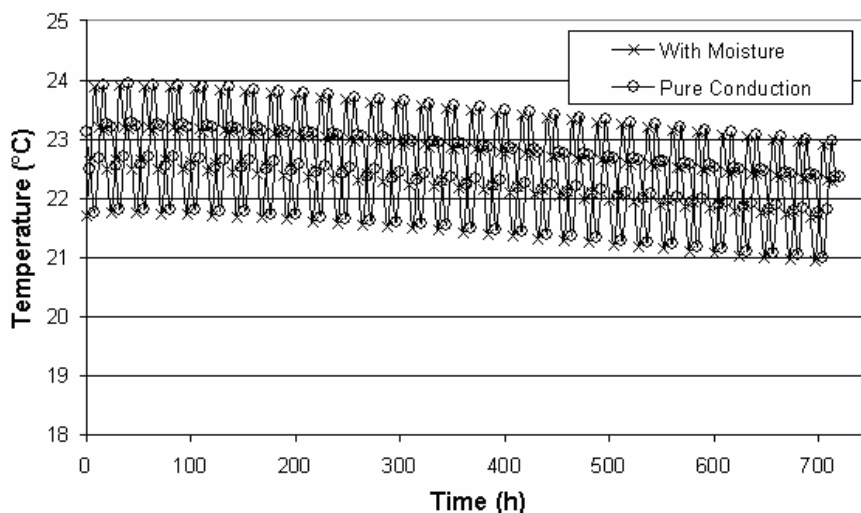


Figure 3: Variation of the internal temperature after 2 years of pre-simulation.

Figure 3 shows the variation of the room air temperature. During the simulation period, it was not verified a significant variation between the purely conductive model and the model that takes moisture transport through the ground and floor into account.

A higher difference of approximately 15% on the internal humidity ratio was verified in Fig. 4, when comparing the “moist” and “dry” models.. It has also been noticed a low daily variation of humidity ratio when moisture is not neglected, *i. e.*, a lower buffer effect of humidity in air occurs when moisture buffer capacity materials are employed.

In the case moisture is disregarded, water vapor is only exchanged by ex- or infiltration. Nevertheless, when moisture is considered, the vapor flow exchanged with the floor can be a significant counterpoise on the room air moisture balance, providing different results in terms of room air

relative humidity. For example, there will be twice as many occupants dissatisfied with the indoor comfort conditions at 24°C and 70% relative humidity than at 24°C and 40%. At the same time, the occupants will perceive the IAQ (Indoor Air Quality) to be better at lower humidity (in fact enthalpy) and recent research results show that ventilation rates could be decreased notably by maintaining a moderate enthalpy in spaces (Hens, 2003).

Furthermore, there is a need to improve the indoor air relative humidity prediction by incorporating accurate moisture models in building thermal simulation programs (Rode *et al.*, 2004). The realization of this need led to formation of an International Research Project, in the framework of the International Energy agency, which started in late 2003 and comprising as many as 19 countries (Hens, 2003).

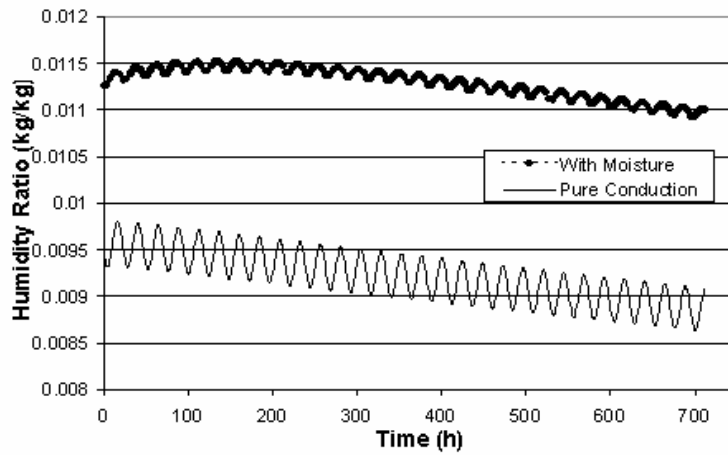


Figure 4: Internal humidity ratio after 2 years of pre-simulation period.

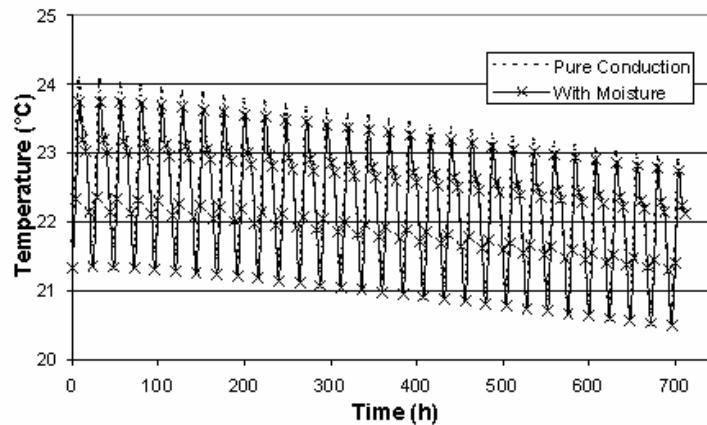


Figure 5: Internal temperature after 2 years of pre-simulation period with an infiltration rate of 10 L/s.

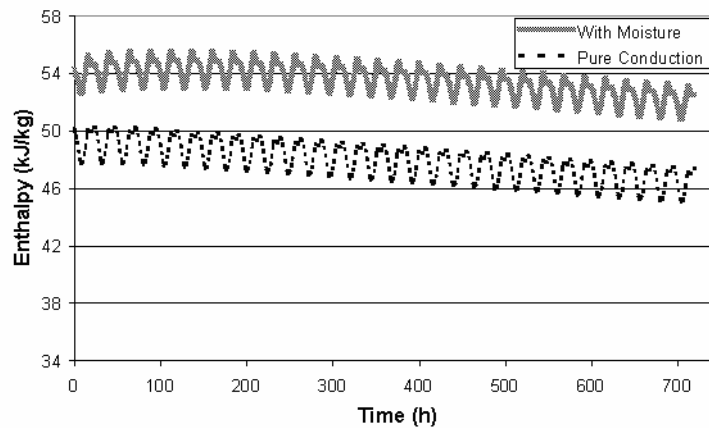


Figure 6: Internal enthalpy after 2 years of pre-simulation period.

Figure 5 shows the evolution of room air temperature when an infiltration rate of 10 L/s is applied. In this case, a maximum difference of 0.5°C was verified between the peak values, attributed to the increase of vapor concentration difference between internal air and floor surface, caused by an increase of the infiltration flow.

The sandy-silt soil moisture effects on indoor temperature are not magnified because soil moisture

increases temperature gradient and transport coefficient due to both water vapor evaporation rate towards the external air and the soil thermal conductivity, which causes a heat loss preferably via the external soil surface. However, in spite of moisture soil effects are not directly perceived by the indoor air temperature, an up to 11% impact on the room moist air enthalpy can be observed in Figure 6. This enthalpy magnification effect can be directly related to HVAC energy consumption.

CONCLUSION

Building simulation codes present some simplifications on their calculation routines of heat transfer through the ground. Regarding the ground heat transfer some aspects should be clarified: the multidimensional phenomenon; the transient behavior and the great number of involved parameters, mainly when moisture is considered.

A review in the literature showed divergences about moisture effects on the ground heat transfer. In addition, most programs do not consider the 3-D asymmetrical effect in the soil.

In this context, a mathematical model has been developed to simulated the hygrothermal performance of single-zone building, considering the combined three-dimensional heat and moisture transport through the ground for capillary unsaturated porous soils under the building. In addition, comparison exercises have been carried out to show how important moisture in soils can be in different scenarios, taking into account the soil hygroscopic parameters.

Concerning the moisture effects on indoor air analysis, slight differences in terms of room air temperature between the purely conductive model for the ground and the moisture model could be noted, due to the importance of solar gains compared to ground heat transfer in the room energy balance and due to the different time scales between room air and soil. However, a significant difference of 15 % was noticed on the room air humidity ratio and 11% on the enthalpy,. Therefore, higher energy consumption could be expected when an air conditioning system is used due to the augmentation of building latent loads.

Besides the energy related aspects, moisture models should be incorporated to building simulation codes due to other indoor relative humidity effects such as perception of indoor air quality, occupant's health and durability of building materials.

Although the moisture effect has caused no significant difference in the room air temperature, obviously a building with a greater area of contact with the ground or in underground zones where the solar radiation effect is not predominant, the moisture flux through the floor could contribute much more effectively for the room air energy balance.

To conclude, some recommendations are addressed for further work: i) Simulation of underground zones and include the moisture effects on the building envelope as well; ii) determination of correlation of ground heat and mass transfer parameters and iii) consideration of a rain model.

ACKNOWLEDGMENTS

The authors thank the Brazilian Research Council (CNPq) of the Secretary for Science and Technology of Brazil.

NOMENCLATURE

A_i - area of the i -th surface (m^2)
 $A_{j,f}$ - area of j -th control volumes of the floor surface discretized by using the finite-volume method (m^2)
 c - specific heat ($J/kg\ K$)
 c_m - mean specific heat ($J/kg\ K$)
 c_w - wall specific heat ($J/kg\ K$)
 c_{air} - air specific heat ($J/kg\ K$)
 D_{Tl} - liquid phase transport coefficient associated to a temperature gradient ($m^2/s\ K$)
 D_{Tv} - vapor phase transport coefficient associated to a temperature gradient ($m^2/s\ K$)
 $D_{\theta l}$ - liquid phase transport coefficient associated to a moisture content gradient (m^2/s)
 $D_{\theta v}$ - vapor phase transport coefficient associated to a moisture content gradient (m^2/s)
 D_T - mass transport coefficient associated to a temperature gradient ($m^2/s\ K$)
 D_θ - mass transport coefficient associated to a moisture content gradient (m^2/s)
 \dot{E}_t - energy flow that crosses the room control surface (W)
 \dot{E}_g - internal energy generation rate (W)
 h_m - mass convection coefficient (m/s)
 h_{mf} - floor mass convection coefficient (m/s)
 h_{ms} - soil mass convection coefficient (m/s)
 h - convection coefficient ($W/m^2\ K$)
 h_{int} - internal convection heat transfer coefficient between internal surfaces and room air ($W/m^2\ K$)
 h_{ext} - external convection heat transfer coefficient between external surfaces and external air ($W/m^2\ K$)
 h_{roof} - external convection heat transfer coefficient for the rooftop ($W/m^2\ K$)
 h_D - the floor massa transfer coefficient ($kg/m^2\ s$)
 H - depth of the ground (m)
 j_v - vapor flow ($kg/m^2\ K$)
 j_l - liquid flow ($kg/m^2\ K$)
 j - total flow ($kg/m^2\ K$)
 L - latent heat of vaporization (J/kg)
 \dot{m}_{inf} - mass flow by infiltration (kg/s)
 \dot{m}_{vent} - mass flow by ventilation (kg/s)
 \dot{m}_b - water vapor flow from the breath of occupants (kg/s)
 \dot{m}_{ger} - internal water-vapor generation rate (kg/s)
 m - number of surfaces

n - number of control volumes of the floor surface discretized by using the finite-volume method

q_r - solar radiation (W/m^2)

R_{lw} - long-wave radiation (W/m^2)

T - temperature ($^{\circ}C$)

T_i - temperature of each surface of the building envelope ($^{\circ}C$)

T_{int} - room air temperature ($^{\circ}C$)

T_{ext} - external air temperature ($^{\circ}C$)

$T_{y=H}$ - temperature of the ground or floor surfaces ($^{\circ}C$)

$T_{x=0}$ - temperature on the external surfaces ($^{\circ}C$)

$T_{x=e}$ - temperature on the internal surfaces ($^{\circ}C$)

T_{prev} - temperature calculated at the previous iteration ($^{\circ}C$)

T_{sur} - temperature of internal surfaces of surrounding walls ($^{\circ}C$)

t - time (s)

V_{air} - room volume (m^3)

W_{ext} - external humidity ratio ($kg\ water/kg\ dry\ air$)

W_{int} - internal humidity ratio ($kg\ water/kg\ dry\ air$)

$W_{v,f}$ - the humidity ratio of each control volume ($kg\ water/kg\ dry\ air$)

α_s - soil solar absorptivity

α_w - wall solar absorptivity

ε_s - soil emissivity

ε_f - floor emissivity

ε_w - wall emissivity

ε_{roof} - roof emissivity

f_v - view factor

ϕ - relative humidity

ϕ_{ext} - external relative humidity

λ - thermal conductivity ($W/m^2\ K$)

λ_f - floor (concrete) thermal conductivity ($W/m\ K$)

λ_s - soil thermal conductivity ($W/m\ K$)

λ_w - wall thermal conductivity ($W/m\ K$)

λ_{roof} - roof thermal conductivity ($W/m\ K$)

ρ - density (kg/m^3)

ρ_0 - solid matrix density (kg/m^3)

ρ_l - water density (kg/m^3)

$\rho_{v,\infty}$ - vapor density in the surrounding air far from the soil surface (kg/m^3)

$\rho_{v,y=H}$ - vapor density at the upper surface of the soil domain (kg/m^3)

ρ_{air} - air density (kg/m^3)

θ - volume basis moisture content (m^3/m^3)

σ - Stefan-Boltzmann constant (W/m^2K^4)

REFERENCES

- ASHRAE – American Society of Heating Refrigeration and Air-Conditioning Engineering - Handbook-Fundamentals Atlanta: ASHRAE, 1997.
- Bahnfleth W. P. 1989. Three-dimensional modelling of slab-on-grade heat transfer, Building Simulation Conference – IBPSA 89, 133-138.
- Davies M., Tindale A., Litter J. 1995. Importance of multi-dimensional conductive heat flow in and around buildings. Building Serv Eng Res Technol, V. 16, 2: 83-90.
- Deru, M. P., Kirkpatrick, A.T. 2002. Ground-coupled heat and moisture transfer from building –Part 2 – Application. Journal of Solar Energy Engineering, 124: 17-21.
- Hens, H. 2003. Proposal for a new annex. Whole building heat, air and moisture response (MOIST-ENG). Katholieke Universiteit Leuven, Belgium.
- Incropera F.P. 1998. Fundamentos de Transferência de Calor e de Massa, 4th ed., LTC Editora.
- Janssen, H., Carmeliet, J., Hens, H. 2002. The influence of soil moisture in the unsaturated zone on the heat loss from building via the ground. Journal of Thermal Envelope and Building Science, Vol. 25, 4: 275-298.
- Mendes, N. 1997. Modelos para previsão da transferência de calor e de umidade em elementos porosos de edificações. Tese de Doutorado. Universidade Federal de Santa Catarina – UFSC.
- Mendes, N., Philippi, P. C., Lamberts, R. 2002. A new mathematical method to solve highly coupled equations of heat and mass transfer in porous media. International Journal of Heat and Mass Transfer, V. 45, 509-518.
- Oliveira Jr, A. A. M., Freitas, D. S., Prata, A. T. 1993. Influência das Propriedades do Meio nas Difusividades do Modelo de Phillip e de Vries em Solos Insaturados. Relatório de Pesquisa. UFSC.
- Patankar S.V. 1980. Numerical heat transfer and fluid flow, Hemisphere Publishing Corporation.
- Perrin B. 1985. Etude des Transferts Couplés de Chaleur et de Masse dans des Matériaux Poreux Consolidés non Saturés Utilisés en Génie Civil", Thèse Docteur d'Etat, Université Paul Sabatier de Toulouse, Toulouse, France.
- Philip, J. R., D. A. de Vries. 1957. Moisture movement in porous media under temperature gradients. Trans Am Geophysical Union, V. 38, 222-232, 1957.
- Rode, C., Mendes N., Grau K. 2004. Evaluation of Moisture Buffer Effects by Performing Whole-Building Simulation, ASHRAE Transactions, USA, 110 (2) 783-794.
- Santos, G. H., Mendes, N. 2004a. Multidimensional Effects of Ground Heat Transfer on the Dynamics of Building Thermal Performance. ASHRAE Transactions. V. 110, 345-354.
- Santos, G. H., Mendes, N. 2004b. Analysis of Numerical Methods and Simulation Time Step Effects on the Prediction of Building Thermal Performance. Applied Thermal Engineering. V. 24, 1129-1142.
- Santos, G. H., Mendes, N. Unsteady Combined Heat and Moisture Transfer in Unsaturated Porous Soils. Journal of Porous Media. V. 8, Issue 6, 2005. (In Press).